

Optical properties of $Zn_{1-x}Fe_xO$ nanoparticles

T.A. Abdel-Baset
taa03@fayoum.edu.eg

Physics Dept., Fac. of Sci., Fayoum University, Fayoum 63514, Egypt.

Abstract— $Zn_{1-x}Fe_xO$ ($x=0,4,6,8,10$) nanoparticles were synthesized using co-precipitation technique at low temperature. X-ray diffraction confirms that the samples have a single-phase wurtzite structure which the bond lengths and the dislocation density increases with an increasing dopant concentration which attributed to the different ionic radii of Fe ions substituted in the ZnO lattice. Optical constant such as optical energy band gap E_g and the reflective index, and the dielectric constant have been determined. The direct optical band gap and the Urbach energy of the $Zn_{1-x}Fe_xO$ NPs decreased with increasing Fe content. The refractive index, the lattice dielectric constant and the optical conductivity are increased with increasing Fe content.

Index Terms— $Zn_{1-x}Fe_xO$ NPs, optical energy band gap, the reflective index, the optical conductivity

1 INTRODUCTION

The most important functional semiconductor materials for optoelectronic devices piezoelectric transducers and gas sensors, is ZnO [1-3], because ZnO is a wide-band gap II-VI semiconductor material, it has a wurtzite-type crystal structure and a direct gap of 3.37 eV at room temperature, and a large exciton binding energy of 60 MeV [4-6]. TM doped ZnO have a technological advantage for their favorable magnetic, the optical and electronic properties required for spintronics materials and optoelectronic devices. [7-18]. Fe doped ZnO nanoparticles have been prepared in different ways, for example, mechanical alloying, Hydrothermal method, solid-state reaction and sol-gel method [19-23]. According to the literature survey, there are many reports of Fe doped ZnO NPs prepared by co-precipitation method. Most of the researcher focus on the ferromagnetic behavior of Fe doped ZnO nanoparticles. However, Fe-doped ZnO can be an important material for uses its optical properties in different applications; thus, it is important to study these properties and the correlation between them. Because the addition of 3d transition metal ions can change the Fermi energy state by raising the valance band maximum and lowering the conduction band minimum, thus reducing the band gap by increasing the concentration of Fe, that is compatible with our results. Thus, it is expected that the doping of Fe metal ion into the ZnO matrix will change the optoelectronic properties as well. In this work, the effects of Fe doped ZnO NPS on the structural and optical properties of ZnO nanoparticles will be studied.

2 EXPERIMENTAL

The preparation of $Zn_{1-x}Fe_xO$ NPs in a nanoparticle form is achieved by using the Co-precipitation technique in our previous essay [24]. Optical characterization was carried out at RT using a Shimadzu UV-3600 UV-vis-near-IR spectrophotometer in the wavelength range 250–800 nm.

3 RESULTS AND DISCUSSIONS

3.1. CHARACTERIZATION

X-ray diffraction pattern of $Zn_{1-x}Fe_xO$ NPs shows that the samples have a single-phase wurtzite structure, with the average particle size 30 nm, and decreases with increasing dopant concentration. This decrease attributed to the small ionic radius of Fe ions compared to that of Zn ions [25]. The effect of doping Fe on the bond length of ZnO nanoparticles was studied. The bond length has been calculated according to the following formula [26]:

$$l = \sqrt{\left(\frac{a^2}{3} + \left(\frac{1}{2} - u\right)^2 c^2\right)} \quad (1)$$

Where a and c are lattice parameters and u is an internal parameter, the bond lengths are given in Table (1). This variation may occurs due to the different ionic radii of Fe ions substituted in the ZnO lattice [27].

Table 1: The XRD data of $Zn_{1-x}Fe_xO$ NPs, the bond length (L) and the dislocation density (δ).

x	$\delta \times 10^{-3} (1/\text{nm})^2$	L(nm)
0	1.014	2.596
0.04	1.141	2.606
0.06	1.231	2.587
0.08	1.126	2.605
0.1	1.173	2.605

The dislocation density (δ), defined as the length of dislocation lines per unit volume of the crystal, is determined by using Williamson and Smallman's relation [28]:

$$\delta = f/D^2 \quad (2)$$

Where f is unity factor, giving a minimum dislocation density.

From Table (1), it is observed that δ increases by increasing the Fe content. This can be attributed to the degradation in crystallinity and the disorder in the ZnO NPs, as a result of the addition of Fe.

3.2 OPTICAL PROPERTIES

3.2.1 OPTICAL BAND GAP AND URBACH ENERGIES OF $Zn_{1-x}Fe_xO$ NPS.

The absorbance spectra of $Zn_{1-x}Fe_xO$ NPs shown in Fig.(1a). It is observed that the absorbance increases with the addition of Fe contents. Also, the optical band gap E_g can be calculated using Tauc's relation [29]

$$(\alpha h\nu) = A(h\nu - E_g)^{1/2} \quad (3)$$

Where α is the absorption coefficient, $(h\nu)$ is the photon energy and A is the probability parameter for transition. This implies that the optical band gap of the ZnO nanostructure has a direct optical transition. It is well known that the direct transitions across the band gap are feasible between the valence and the conduction band edges in k-space. In this transition process, the total energy and momentum of the electron-photon system must be conserved.

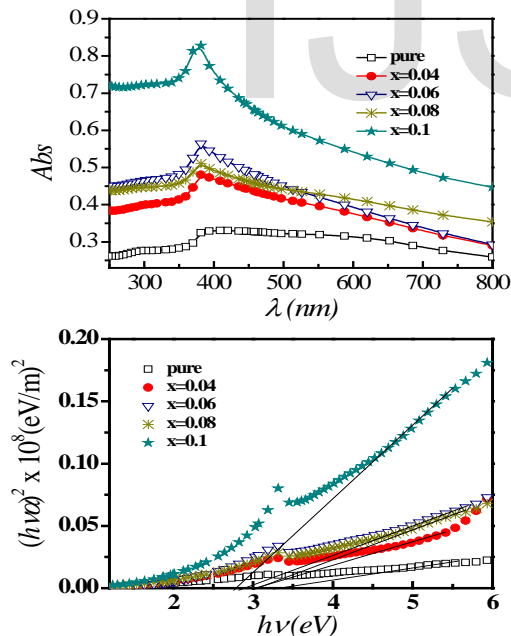


Fig. 1: (a) The main frame represents UV-vis absorption spectra, and (b) shows the plots of $(\alpha h\nu)^2$ versus $h\nu$.

The direct band gap were obtained from plots of $(\alpha h\nu)^2$ versus $h\nu$ at RT enables us to estimate the E_g values by extrapolating the linear part of $(\alpha h\nu)^2$ to zero as shown in Fig.(1b),

and the obtained E_g values are tabulated in Table 2. The optical band gap shifted slightly to lower energies than that of the pure ZnO. Thus, in our samples, the s-d and p-d exchange interactions give rise to a negative and a positive correction to the conduction and the valence band edges, respectively which reduced the band gap by adding Fe content [30-32].

Table 2. The direct energy band gaps, Urbach energies and the dispersion parameters for $Zn_{1-x}Fe_xO$ NPs.

x	E_g (eV)	E_U (eV)	ϵ	$\left(\frac{e^2}{\pi c^2}\right)\left(\frac{N}{m^3}\right)*10^{-6}$
0.0	3.28	2.18	7.63	3.74
0.04	3.06	1.6	9.43	5.70
0.06	2.94	1.48	10.03	6.57
0.08	2.92	2.53	10.05	6.37
0.1	2.79	2.84	13.88	7.59

The absorption coefficient near the fundamental absorption edge is exponentially dependent on $h\nu$ and obeys the empirical Urbach relation, the Urbach energy can be calculated according to the following relation [33]

$$\alpha = \alpha_0 \exp\left[\frac{h\nu - E_U}{E_U}\right] \quad (4)$$

Where E_U and α_0 are constants and E_U is the Urbach energy which refers to the width of the exponential absorption edge. Eq. (4) describes the optical transition between occupied states in the valence band tail to unoccupied states of the conduction band edge. E_U values were calculated from the slopes of the graphs shown in Fig.2, using the relationship $E_U = (d \ln \alpha / h\nu)^{-1}$, and given in Table 2.

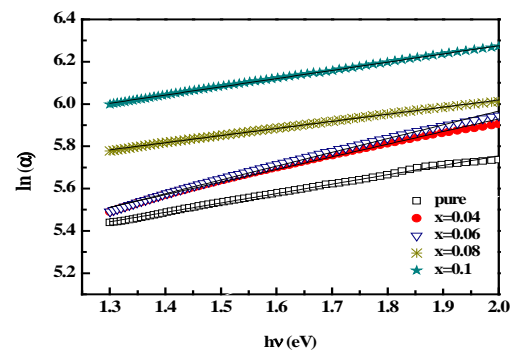


Fig.2: $\ln(\alpha)$ versus $h\nu$.

The increase of E_U suggests that the atomic structural disorder of $Zn_{1-x}Fe_xO$ NPs increases by Fe doping. This decrease would lead to a redistribution of states from the band to the tail, allowing a large number of possible band to tail and tail to tail transitions [34].

3.2.2 REFRACTIVE INDEX DISPERSION

The refractive index plays an important role in optical communication and designing of the optical devices. The refractive index (n) can be calculated as follows[35] :

$$n = \left(\frac{1+R}{1-R} \right) + \sqrt{\frac{4R}{(1-R)^2} - k^2} \quad (5)$$

Where the reflectance (R) given by $[R = 1 - \sqrt{(T * \exp(A))}]$ and the extinction coefficient, k , ($k = \alpha\lambda/4\pi$) Fig.3. shows the refractive index distributions of $Zn_{1-x}Fe_xO$ NPs. The values of n are tabulate in the table 2, the values of the refractive index are found to increase with the addition of Fe. Such increase in n may extend the usability of these materials as antireflection coating.

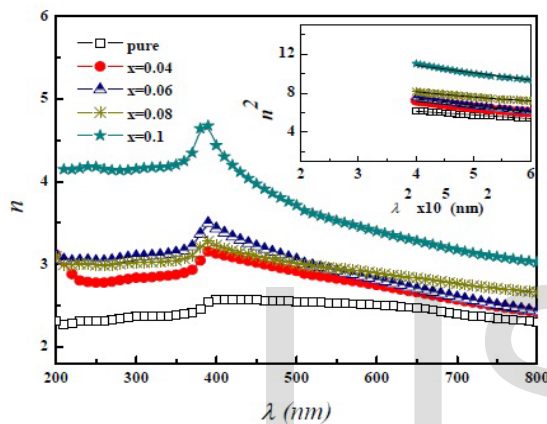


Fig. 3: The variation in refractive index (n) versus wavelength (λ), and the inset shows the plots of n^2 vs. λ^2

The values of the lattice dielectric constant (ϵ) and the ratio of carrier concentration to the electron effective mass ($(e^2/\pi C^2)(N/m^*)$) can be calculated by considering the dependence of n^2 on λ^2 (in the inset Fig. 3) according to the following dispersion relation [36]:

$$n^2 = \epsilon - \left(\frac{e^2}{\pi C^2} \right) \left(\frac{N}{m^*} \right) \lambda^2 \quad (6)$$

The values of these parameters are shown in Table2. The values of the dielectric constant increased with increasing Fe content, and the ratio of carrier concentration to the electron effective mass increased also, this means that Fe content increases the charge carrier concentration, this is consistent with the decrease in E_g with increasing Fe content also with the XRD results where the crystallinity enhancement is related to the defects and charge carriers [37].

3.2.3 THE OPTICAL CONDUCTIVITY OF $Zn_{1-x}Fe_xO$ NPs

The optical conductivity means the electrical conductivity results from the movement of the charge carriers due to alternating electric field of the incident electromagnetic waves [38]. The real part represents the in-phase current, while the imaginary part represents the $\pi/2$ out of-phase inductive current. The real (σ_1) and imaginary (σ_2) components of optical conductivity are described as [39,40]

$$\sigma_1 = \omega \epsilon'' \epsilon_0, \quad \sigma_2 = \omega \epsilon' \epsilon_0 \quad (7)$$

Where ω is the angular frequency and ϵ_0 is the free space dielectric constant. The real σ_1 and the imaginary σ_2 parts of the optical conductivity for $Zn_{1-x}Fe_xO$ NPs are shown in Fig. (4a, 4b). The values of the imaginary part of the optical conductivity are larger than that of the real part of optical conductivity. Also, it can be seen that both of the two parts of the optical conductivity values vary with Fe content as the optical properties of s are strongly influenced by their structural characteristics. According to these results, it can be suggested that all of these optical parameters for $Zn_{1-x}Fe_xO$ NPs will be changed with Fe content and could be used in optical devices and optoelectronic applications.

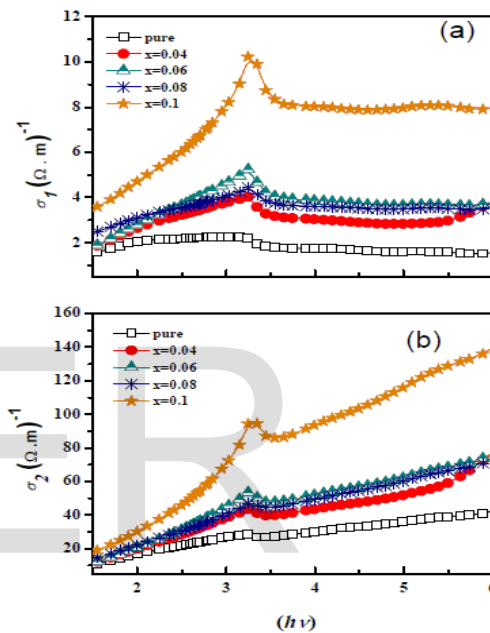


Fig.4: (a) The real parts, and (b) The imaginary part of the optical conductivity versus $h\nu$.

4 CONCLUSION

The bond lengths and the dislocation density increases with the increase of the dopant concentration. The direct optical band gap and the Urbach energy of the $Zn_{1-x}Fe_xO$ NPs decreased with increasing Fe content. Also the optical constants were determined and these parameters were changed with Fe dopant. The refractive index and the carrier concentration to the electron effective mass increased. The lattice dielectric constant and the optical conductivity are increased with increasing Fe content. Based on these results, the $Zn_{1-x}Fe_xO$ NPs would be a promising candidate for various optoelectronic applications.

REFERENCE:

1. Xu W. Z., Ye Z. Z., et al (2009) . Appl. Phys. Lett. 88: 173506-173509.
2. Tu Z. C., Hu X., (2006) Physical Review B, 74, 035434.
3. Mitra P., Chatterjee A. P., Maiti H. S., (1998) Materials Letters, 35: 33-38.
4. Mang A., Reimann K., Rubenacke St. (1995) Solid State Commun. 94: 251.
5. Srikant V., Clarke D. R., (1998) J. Appl. Phys. 83: 5447.
6. Djurisc A. B., Chen X., et al (2012) . Journal of Materials Chemistry, 22: 6526.
7. Liu M., Kitai A. H., Mascher P.,(1992) Journal of Luminescence 54: 35.
8. Ueda K., Tabat H., Kawai T. (2001) Applied Physics Letters, Vol. 79: 988.
9. Risbud A. S., Spaldin N. A., et al (2003) Physical Review B, 68: 205202.
10. Pearton S. J., Abernathy C. R., et al (2003) J. Appl. Phys. 93: 1-13.
11. Lawes G., Risbud A. S. et al (2005) Physical Review B 71: 045201.
12. Rao C. N. R., Deepak F. L.,(2005) Journal of Materials Chemistry, 15: 573.
13. Thota S., Dutta T., Kumar J., (2006) Journal of Physics: Condensed Matter, 18: 2473-2478.
14. Ungureanu M., Schmidt H.,et al (2007) Thin Solid Films, 515: 8761.
15. Wang Q., Geng B., Wang S.,(2009) Environ. Sci. Technol. 43: 8968-8973.
16. Zhou Y., Lu S. X., Xu W. G.,(2009) . Environmental Progress & Sustainable Energy, 28: 226.
17. Yang L., Jinghai Y, et al.(2009) Journal of Alloys and Compounds 486: 835.
18. Li F., Yuan Y., et al (2010) Applied Surface Science, 256: 6076.
19. Lin Y., Jiang D., et al, (2007) Fe-doped ZnO magnetic semiconductor by mechanical alloying J. Alloys Compd. 436: 30.
20. Wu X. Wei Z., et al,(2014) , Journal of Nanomaterials ,1- 6.
21. Ahn G.Y., Park S.I., et al,(2005)IEEE Trans. Magn. 41:2730.
22. Ahn G.Y., Park S.I., Kim C.S.,(2006)) J. Magn. Magn. Mater. 303: 329.
23. Beltrán J. J. , Barrero C.A., Punnoose A. (2015) Phys. Chem. 17: 15284.
24. Abdel-Baset T. A., Fang Y. W., et al. (2016) Nanoscale Research Letters, 11:115.
25. Mishra A.K, Das D., (2010) Mater Sci Eng B, 171: 5.
26. Pan Z., Xiao Y. et al (2014), Mater. Sci. Semicond. Process. 17: 162.
27. Karamat S., Rawat R.S., et al, (2014) Progress in Natural Science: Materials International 24, 142.
28. Ivanova T., Harizanova A., et al, (2010) Mater. Lett. 64:1147.
29. N. Reddeppa, A.K. Sharma, et al, (2013) Microelectron. Eng. 112: 57.
30. Diouri J., Lascaray J. P., El Amrani M. (1985) Phys. Rev. B, 31: 7995.
31. Bylsma R. B., Becker W. M., et al (1986) Phys. Rev. B 33: 8207.
32. Ando K., Saito H.,(2001) Appl. Phys. Lett. 89: 7284.
33. Urbach F.,(1953) Phys. Rev. 92: 1324.
34. O'Leary S.K., Zukotynski S., Perz J.M.,(1997) J.Non Cryst. Solids 210:249.
35. Yahia I. S., Farag A. A. M. , et al ,(2013) Super lattices Microstruct. , 53: 63.
36. El-Sayed S., Abel-Baset T., et al. (2015) Physica B 464: 17.
37. Ali H.M., Mohamed H.A., et al, (2007) Thin Solid Films 515 (2007) 3024
38. Mariappan R., Ponnuswamy V.,et al (2013) Super lattice. Microst. 59: 47.
39. J.N. Hodgson, (1970)"Optical Absorption and Dispersion in Solids", Chapman and Hall Ltd, London.

Broza G., Piszczek K., et al, (2007) composites Sci. and Tech., 67: 890

